NASA
Technical
Paper
2181

August 1983

Investigation of Jet-Installation Noise Sources Under Static Conditions

John G. Shearin

NASA

25th Anniversary
1958-1983

NASA
Technical
Paper
2181

1983

Investigation of Jet-Installation Noise Sources Under Static Conditions

John G. Shearin
Langley Research Center
Hampton, Virginia

NASA
National Aeronautics
and Space Administration

Scientific and Technical
Information Branch

SUMMARY

The acoustical effects of operating a 6-cm exit-diameter nozzle in the presence of a wing-flap model under static conditions are examined experimentally. The geometric parameters of the wing-flap model are chosen to represent a realistic jet-engine installation on a wide-body midrange transport airplane. The effects of varying the installation parameters and the noise sources associated with the engine-installation effects are discussed.

Based on the results, it is concluded that the major noise source in the low-frequency region is the flow interaction of the jet and wing undersurface. The major noise source in the midfrequency region is the flow interaction of the jet with the side edges of the flap cutout. An additional noise source in this frequency region is the flap trailing edge which dominates in the absence of the flap cutout. The high-frequency-region noise source is primarily due to jet noise reflecting off the undersurface of the wing and flap. Also, the jet impinging on the flap cutout contributes to the high-frequency-region noise when the cutout size is smaller than the local jet diameter.

INTRODUCTION

One of the problems in reducing airplane flyover noise today is identifying the various sources of noise radiated from an installed engine. Sources other than direct engine-exhaust noise or turbomachinery noise are referred to as installation effects and can be manifested in two broad categories. The first is the acoustic interaction involving the modification of sound, radiated from jet exhaust, by an airplane structure such as the wing, fuselage, and flaps. The second is the aerodynamic interaction resulting from the modification of a jet structure by the proximity of the wing undersurface and direct interaction between the jet and flaps.

The acoustic interaction has been the subject of many investigations. (See refs. 1 through 7.) Reference 1 investigated the wing effect on propagation of jet noise, which showed that the presence of the wing in the vicinity of the jet increased the noise over that of the jet alone. A theoretical model for reflection and edge diffraction of jet noise due to the presence of a wing or high vertical stabilizer was the subject of reference 2. Reference 3 contains the results of an investigation of the noise generated by a small model of a double-slotted, externally blown flap. References 4 and 5 present a comprehensive study on the generation of sound resulting from the passage of a turbulent jet over a flat plate of finite dimensions. These two studies showed the dependence of the acoustic far field on the dimensions of the plate, the distance between the jet axis and the plate, and the velocity of the jet. Reference 6 discusses the effects of forward motion on jet noise. This study found that for airplanes with engines mounted under the wing and with flap deflections greater than 30°, the additional contribution from the jet-flap-interaction noise was as much as 5 dB and was responsible for higher in-flight, low-frequency noise levels during approach conditions than airplanes without flap deflections. Models of wide-body airplanes were used in reference 7 to investigate the increased noise brought about by installing a turbofan engine under an airplane

wing. Both reflection of the jet noise from the wing undersurface and interaction noise generated from the deployment of the flaps into the jet exhaust were experienced.

The acoustic interaction and the aerodynamic interaction will vary from one airplane to another. However, current midrange transports have flap systems that protrude into the jet exhaust when deflected; thus, the aerodynamic interaction with the jet exhaust is a problem of general interest. Since the noise sources of engine installation effects are not well understood and the noise sources are not identified, this study was conducted to identify the noise sources related to the geometry of a jet-wing-flap system.

This report describes the noise sources from operating a 6-cm exit-diameter nozzle in the presence of a wing-flap model under static conditions (no forward velocity). Three geometric installation parameters and the flap-deflection angle were investigated: (1) the normal distance between the jet center line and the wing chord, (2) the normal distance between the nozzle exit and the deflected-flap trailing edge, and (3) the width of the flap cutout which is generated by the deflected-flap system and allows the jet to pass through. These parameters were chosen to represent the range of values associated with current midrange, wide-body transport airplanes.

SYMBOLS

Values are given in SI Units and, where considered useful, also in U.S. Customary Units.

D	nozzle-exit diameter, cm
f	1/3-octave-band center frequency, Hz
H	normal separation distance between jet center line and wing chord, cm
L	normal distance between nozzle exit and flap trailing edge ($\delta = 0°$), cm
R	distance between far-field observation point and model, m
V	jet center-line velocity, m/s
W	width of flap cutout, cm
δ	flap-deflection angle, deg
θ	observation angle measured from jet downstream axis in plane perpendicular to wing flap, deg

Abbreviations:

FM	frequency modulation
ips	inches per second
Mic	microphone

OASPL overall sound pressure level, dB

ΔOASPL difference between static and flight noise levels, dB

SAE Society of Automotive Engineers

SPL sound pressure level, dB (referenced to 20 μPa)

FACILITY AND TEST APPARATUS

The test was conducted in the Langley Anechoic Noise Facility. The anechoic chamber of the facility is approximately 7.6 m long, 7.6 m wide, and 7.0 m high measured between wedge tips. The walls, floor, and ceiling are lined with foam and fiberglass wedges, which were designed for a chamber cutoff frequency of approximately 100 Hz. Sound-pressure measurements at distances up to approximately 5 m are possible by means of a microphone boom over an arc of 135°. The air system has the capacity to supply dry air at pressures up to 1551 kPa (225 psig) and at flow rates up to 4.5 kg/s (10 lb/s) to the nozzle. Control valves, mufflers, and a settling chamber are provided to assure quiet airflow for jet-nozzle experiments. An overhead eductor-inductor system is provided for passage of air in or out of the test area. Additional information on this facility is contained in reference 8.

A photograph of the experimental apparatus in the anechoic room is shown in figure 1. Air from a regulated high-pressure system was supplied continuously into a 0.57-m-long pipe, which formed the 6-cm-diameter nozzle. This nozzle was chosen because its aerodynamic characteristics were well-documented in reference 9. The minimum operating Reynolds number based on the nozzle diameter was 6×10^5, which was considered suitable for modeling a typical turbofan primary-exhaust diameter. In addition, the length of the nozzle was suitable for mounting the test model.

Since the wing and flap system (including installation parameters) are the main components affecting the noise characteristics for an underwing engine, the dimensions of these components and the range of values of the installation parameters were carefully chosen to represent a typical transport airplane. An NACA 0012 symmetrical airfoil with a 0.31-m chord and 0.61-m span was used for the wing, as well as for the flaps which had 8.9-cm chords. The supporting system for the wing and flap consisted of side plates for rigidity, which were constructed with enough clearance so as not to interact with the jet. (See fig. 2.) The support system also provided adjustments to position the trailing edge of the flap relative to the nozzle exit and to determine the flap-deflection angle. A series of flaps with cutouts ranging from 5.1 cm to 11.4 cm were used to evaluate the influence of the cutouts on the jet-exhaust noise. A flap with no cutout was also tested and used to determine the importance of the trailing-edge noise. Details of these flaps are shown in figure 3. Additional diagnostic measurements using a flat plate were also conducted to aid in determining the noise sources.

INSTRUMENTATION AND PROCEDURES

Twelve 1/2-in. condenser microphones were located in an arc, with a radius of 3.7 m at 10° intervals between observation angles (θ) of 20° and 130° from the jet downstream axis. The arc was in a plane perpendicular to the wing surface. (See fig. 1.) However, only data for $\theta \geq 50°$ are presented in this report because the microphones with $\theta < 50°$ were in the jet flow. In addition, four surface-pressure

sensors (two each on the upper and lower surface, see fig. 3) were embedded in one flap near the edge of the cutout to measure the surface-pressure fluctuations. Data from these transducers are used to aid in determining the noise source in the low-frequency regions. Data from all microphones were recorded by an FM tape recorder at 60 ips (in/s) and were also evaluated on-line with a 1/3-octave-band real time spectral analyzer. The 1/3-octave data were stored on a computer disk. An interactive graphics terminal was used to monitor the experiment and to display acoustic data.

The four geometric test parameters investigated are shown in figure 4. These four parameters are all interrelated because of the flow properties that influence the noise radiation from the jet, and the jet-flap interaction includes the local jet diameter, the local center-line velocity, and the local maximum turbulent intensity. Changes in these flow quantities can be achieved by a number of different combinations of the geometric test parameters. Thus, all possible combinations of these test parameters were investigated at jet velocities of 152, 183, and 244 m/s or Mach numbers of 0.44, 0.53, and 0.71, respectively. The following table lists the nondimensional values of these test parameters:

H/D	L/D	W/D
1	3.6	0
2	5.5	.84
		1.3
		1.5
		1.7
		1.9

RESULTS AND DISCUSSION

In this section, the free-jet noise spectra are presented as base-line data, and the frequency range for all data is divided into three different regions in order to define the dominant frequency bands of the noise sources. In addition, the test parameters that affect these sources are identified. Data are also presented that indicate the superposition of two noise sources that exist in one of the frequency regions. Lastly, a comparison between jet-flap-interaction noise and jet-impingement noise is presented. These results are supported by graphs in the form of overall sound pressure level (OASPL), 1/3-octave-band sound-pressure-level (SPL) spectra, and directivities.

Free-Jet Base-line Data

Figure 5 describes the measured free-jet noise spectra for the test velocities of 152, 183, and 244 m/s or Mach numbers of 0.44, 0.53, and 0.71, respectively. Included in this figure is the predicted noise spectrum of the Society of Automotive Engineers (SAE) for a velocity of 152 m/s. The calculated and measured noise spectra at this velocity are similar in shape. However, the SAE overpredicts approximately by 2 to 3 dB across the frequency range. This is due to the fact that the engine data used for determining the SAE noise-prediction program have relatively large scatter at Mach numbers less than 0.71. (See ref. 10.) The OASPL of the free jet followed a jet velocity to the eighth power. Figure 5 also describes the three

frequency (f) regions of interest, which are low (100 Hz < f < 800 Hz), middle (800 kHz < f < 5 kHz), and high (5 kHz < f < 20 kHz).

Sources of Jet-Flap-Interaction Noise

The take-off requirement of a midrange wide-body transport with engines mounted under the wing requires the engines to be close to the wing undersurface, and landing requirements dictate a large flap deflection. The relative location of the flap and the undersurface of the wing with the exhaust (jet) of the engine will cause a strong interaction between the flap and jet. Figure 6 illustrates a possible location of the trailing edge and side edge of the flap relative to a typical turbulent jet. Where a flap cutout does not exist and the flap is not deflected, there is a weak interaction between the trailing edge and the turbulence. As the flap is deflected, the trailing edge protrudes into a varying region of turbulence intensity and a strong interaction exists at a large flap deflection.

In a flap cutout condition in which the local jet diameter is larger than the cutout and a large flap deflection exists, more cutout side edge is in the turbulent region, thus resulting in a strong interaction. The relative position of the engine nozzle exit with the flap can also produce a weak or strong jet-flap interaction. It will be weak if the exit is close to the flap cutout because the jet diameter will be smaller as it passes through the cutout. If the jet is fully developed, the local jet diameter will be much larger than the flap cutout width, thus causing a strong interaction. Also, the turbulent region of the jet is long relative to the wing chord, which results in a strong jet interaction with the wing.

Low-frequency noise source.- The noise generated in the low-frequency region (100 Hz < f < 800 Hz) is primarily due to the interaction of the jet and wing. This is seen in figure 7 where the wing is removed and only the deflected flap remains. With the wing removed, the low-frequency noise spectrum is reduced to approximately that of the free jet with the exception of the highest end of the low-frequency region. Further evidence that the noise generated in the low-frequency region is due to the jet-flow—wing interaction can be observed in figure 8. This figure shows the pressure spectra measured by flush-mounted pressure transducers on the upper and lower flap surfaces near the flap cutout edge. (See fig. 3.)

In the low-frequency region, the two spectra differ significantly in magnitude; however, in the midfrequency region, they have the same spectral shape and peak frequency. The upper-surface pressure transducer is shielded by the flap from the jet-flow—wing interaction and responds primarily to the local jet-flow—flap interaction, whereas the lower-surface microphone senses both flow interactions. Evidence that the upper-surface transducer responds primarily to the jet-flow—flap interaction can be observed in figure 9. This figure shows the superposition of the far-field noise spectrum of the jet and flap with the wing removed and the upper-surface pressure spectrum with jet, wing, and flap. The peak noise of the two spectra differ by 50 dB; thus, the magnitude of the two spectra are not relative but are similar in spectral shape and peak frequency. Based on figures 7, 8, and 9, the primary low-frequency noise source is the interaction of the jet near field with the wing. The aerodynamic process involved could be the modification of the jet-mixing development by the modified-flow entrainment.

If the aforementioned is true, then the most important parameter in the low-frequency region is H/D since, if H/D is large enough, no interaction exists. This can be concluded from figure 10 where the normal distance H has the values of

one and two nozzle-exit diameters, and all other parameters are constant. This figure shows that the low-frequency noise level increases as the distance H is decreased.

For H/D values where interaction exists, the jet entrainment would depend on the geometry of the jet-nozzle placement relative to the wing. Thus, L/D should influence this low-frequency noise, as shown in figure 11. This figure shows that the SPL in the low-frequency region increases as the distance L is increased.

If the source is mainly the jet-entrainment modification by the wing surface, then it should be relatively insensitive to the details of flap geometry. Figure 12 shows that the low-frequency noise is basically insensitive to the flap deflection for W/D = 0. Figure 13 indicates that the low-frequency noise is sensitive to the flap deflection with W/D = 0.84. However, this could be due to the fact that some low-frequency noise component is also generated as a result of jet-flow—flap cutout side-edge interaction. Further evidence that the low-frequency noise is due to jet-wing interaction is seen in figure 14 ($\delta = 40°$, W/D = 0), where the peak SPL in the low-frequency region varies as V^3 and not V^6, a result which characterizes edge noise.

Midfrequency noise source.- The noise source for the midfrequency region (800 kHz $\leq$ f < 5 kHz) is the jet-flow—flap interaction. This can be determined from figures 7 and 9. Figure 7 shows the noise spectra obtained for the wing-flap model and the flap alone (wing removed). In the midfrequency region, the two noise spectra are similar, thus indicating that the primary noise source is the flap. Figure 9, previously discussed in the section entitled "Low-Frequency Noise Source," indicates the same conclusion. The primary feature of this type of noise source should have a V^6 dependency. Such a dependency is shown in figure 15, which shows the effects of jet velocity on the peak sound pressure level in the midfrequency region, where the flap is deflected 40° and the flap cutout ratio is 1.3.

The side edges of the flap cutout should also be a noise source in the midfrequency region. Figure 16 shows the importance of the side edges of the cutout. As W/D increases, the nature of the jet-flap interaction reduces to a weak interaction, since the impingement on both the trailing edge and side edges has been reduced appreciably. Thus, it appears there is no basic difference in the midfrequency noise generated at the trailing edge and side edges. This noise basically depends on the local turbulence level (proportional to the local mean velocity) existing at those edges.

High-frequency noise source.- The high-frequency region is defined to be 5 kHz < f < 20 kHz. It is limited to 20 kHz since that is the frequency where the microphone response ceased to be a linear response. From figure 12 it is obvious that there is considerable high-frequency noise generation for the case of strong interaction between the jet and the flap when $\delta = 40°$. This high-frequency noise reduces to approximately 3 dB above the free-jet noise when the flap cutout width is increased to approximately the size of the local jet diameter (W/D = 1.5). (See fig. 16.) The identical phenomenon results when the flap deflection is reduced to zero. Thus, the strong interaction with flow impinging on the flap and the flap cutout side edges is a noise source in the high-frequency region.

When the conditions are such that the flow-impingement noise and flap cutout side-edge noise do not exist in the high-frequency region (see fig. 17), the noise source in this region is reduced primarily to reflections of the jet noise. These reflections, which are observed from the data presented in figure 18, are due to the presence of the wing undersurface. Figure 18 represents the 1/3-octave-band noise spectrum of the jet, wing, and nondeflected flap compared with the noise spectrum when the wing is removed. In the high-frequency region, the SPL for the wing and flap is approximately 3 dB above the free-jet noise; whereas with the wing removed, the SPL is reduced to that of the free jet because of an absence of the reflecting surface of the wing.

Figure 19 shows the dependency of the reflected jet noise on the observation angle θ. In this figure, ΔOASPL is the amount the spectra for the wing and flap exceed that of the free jet in the high-frequency region. The increase attributed to reflected noise is not observed until $\theta > 60°$. Figure 19 also illustrates that high-frequency noise is nearly independent of the jet center-line velocity.

Superposition of Spectra in Midfrequency Region

When the flap deflection angle δ is 0° and the flap-cutout width W is 0, a 1.25-kHz narrow-band peak SPL occurs. Figure 20 shows the 1/3-octave-band noise spectra for this configuration with the jet noise subtracted and with a variation in jet velocity. The peak SPL in the midfrequency region does not shift in frequency with a change in jet velocity. This, at first sight, indicates that the origin of the peak SPL is unrelated to the aerodynamic interaction. Narrow-band analysis of the same data was performed to see if the observed 1/3-octave-band peaks were discrete emissions, and the results are presented in figure 21. It is seen that the peak at 1.25 kHz is not a pure tone. In addition, an accelerometer was attached to the upper surface of the flap, and the results showed that the peak SPL was not due to structural vibrations.

It was reasoned that the apparent independence of the midfrequency noise with velocity could be due to the superposition of two source spectra: the jet-wing and jet-flap interactions, where each source has its own dependence on V and its own Strouhal scaling. The net result of the superposition of these two component spectra could be an apparent independence of peak frequency with V.

Narrow-Band Peak in High-Frequency Region

When the solid flap is deflected 40°, a narrow-band peak SPL at 6.3 kHz for $L/D = 5.5$ and 3.6 is observed as noted earlier in figure 12. Narrow-band analysis showed that this peak is not a tone. When a cutout is made on the flap, the peak at 6.3 kHz disappears, as observed in figure 16. In order to determine the source of the peak SPL at 6.3 kHz, the wing was removed which left only the deflected flap, and also a slanted flat plate was used instead of the flap. In both cases, the peak SPL at 6.3 kHz was not present as seen from figure 22. Thus, the SPL peak at 6.3 kHz is most likely due to the nonturning flow at the location where the wing and deflected flap intersect. At this location, the flow tends to recirculate, which produces the

subject peak SPL. The following sketch shows a typical recirculating flow where the wing and flap intersect:

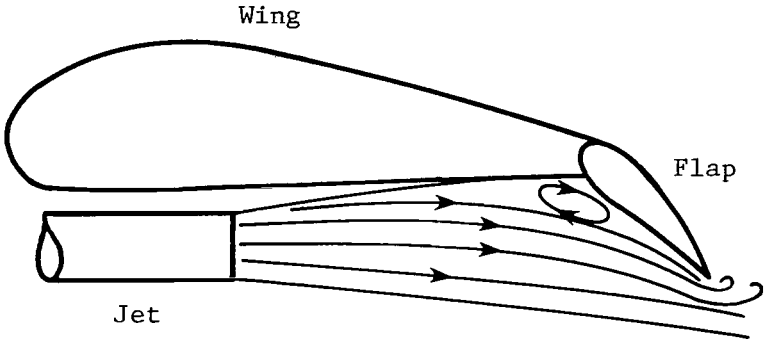

Comparison Between Jet-Flap-Interaction Noise and Jet-Impingement Noise

In addition to the noise spectra for a slanted flat plate and a deflected flap with no wing, the noise spectrum for a nondeflected flap with no wing is presented in figure 22. An interesting observation is that when the flap is deflected, the impinging jet not only increases the high-frequency SPL but also increases the low-frequency SPL. The effect is stronger for the flat plate, where the flow impingement can cause flow reversal and subsequent flow separation in the upstream portion of the impingement region. It is believed that the subsequent flow separation increases the low-frequency SPL.

CONCLUDING REMARKS

The effects of operating a 6-cm exit-diameter nozzle in the presence of a wing-flap model under static conditions has been investigated experimentally in the Langley Anechoic Noise Facility. The installation parameters of the jet-flap model were chosen to provide a realistic geometric simulation of an actual jet-engine installation. Effects of varying the installation parameters were determined and discussed, and the noise sources for engine installation effects are defined.

Based on the results obtained in the present study, it is concluded that the major noise source in the low-frequency region is the flow interaction of the jet and wing undersurface. The major noise source in the midfrequency region is the flow interaction of the jet with the side edges of the flap cutout. An additional noise source in this frequency region is the flap trailing edge which dominates in the absence of the flap cutout. The high-frequency-region noise source is primarily due to jet noise reflecting off the undersurface of the wing and flap. Also, the jet impinging on the flap cutout contributes to the high-frequency-region noise when the cutout size is smaller than the local jet diameter.

Increasing the normal separation distance H between the wing chord and the jet center line decreases the noise levels. Increasing the normal distance L between

the nozzle exit and the flap trailing edge increases the noise levels. Large flap deflections increase the noise levels, and an increase in the flap cutout width results in a decrease in the noise level.

Langley Research Center
National Aeronautics and Space Administration
Hampton, VA 23665
July 12, 1983

REFERENCES

1. Wang, M. E.: Wing Effect on Jet Noise Propagation. AIAA-80-1047, June 1980.

2. Southern, I. S.: Exhaust Noise in Flight: The Role of Acoustic Installation Effects. AIAA-80-1045, June 1980.

3. Olsen, William A.; Dorsch, Robert G.; and Miles, Jeffrey H.: Noise Produced by a Small-Scale Externally Blown Flap. NASA TN D-6636, 1972.

4. Grosche, F. R. (D. G. Randall, transl.): On the Generation of Sound Resulting From the Passage of a Turbulent Air Jet Over a Flat Plate of Finite Dimensions. Library Trans. No. 1460, British R.A.E., Oct. 1970.

5. Head, R. W.; and Fisher, M. J.: Jet/Surface Interaction Noise:- Analysis of Far-field Low Frequency Augmentations of Jet Noise Due to the Presence of a Solid Shield. AIAA Paper No. 76-502, July 1976.

6. Low, J. K. C.: Effects of Forward Motion on Jet and Core Noise. AIAA Paper No. 77-1330, Oct. 1977.

7. Way, D. J.; and Turner, B. A.: Model Tests Demonstrating Under-Wing Installation Effects on Engine Exhaust Noise. AIAA-80-1048, June 1980.

8. Hubbard, Harvey H.; and Manning, James C.: Aeroacoustic Research Facilities at NASA Langley Research Center - Description and Operational Characteristics. NASA TM-84585, 1983.

9. Maestrello, L.; and McDaid, E.: Acoustic Characteristics of a High-Subsonic Jet. AIAA J., vol. 9, no. 6, June 1971, pp. 1058-1066.

10. Bushell, K. W.: A Survey of Low Velocity and Coaxial Jet Noise With Application to Prediction. J. Sound & Vib., vol. 17, no. 2, July 22, 1971, pp. 271-282.

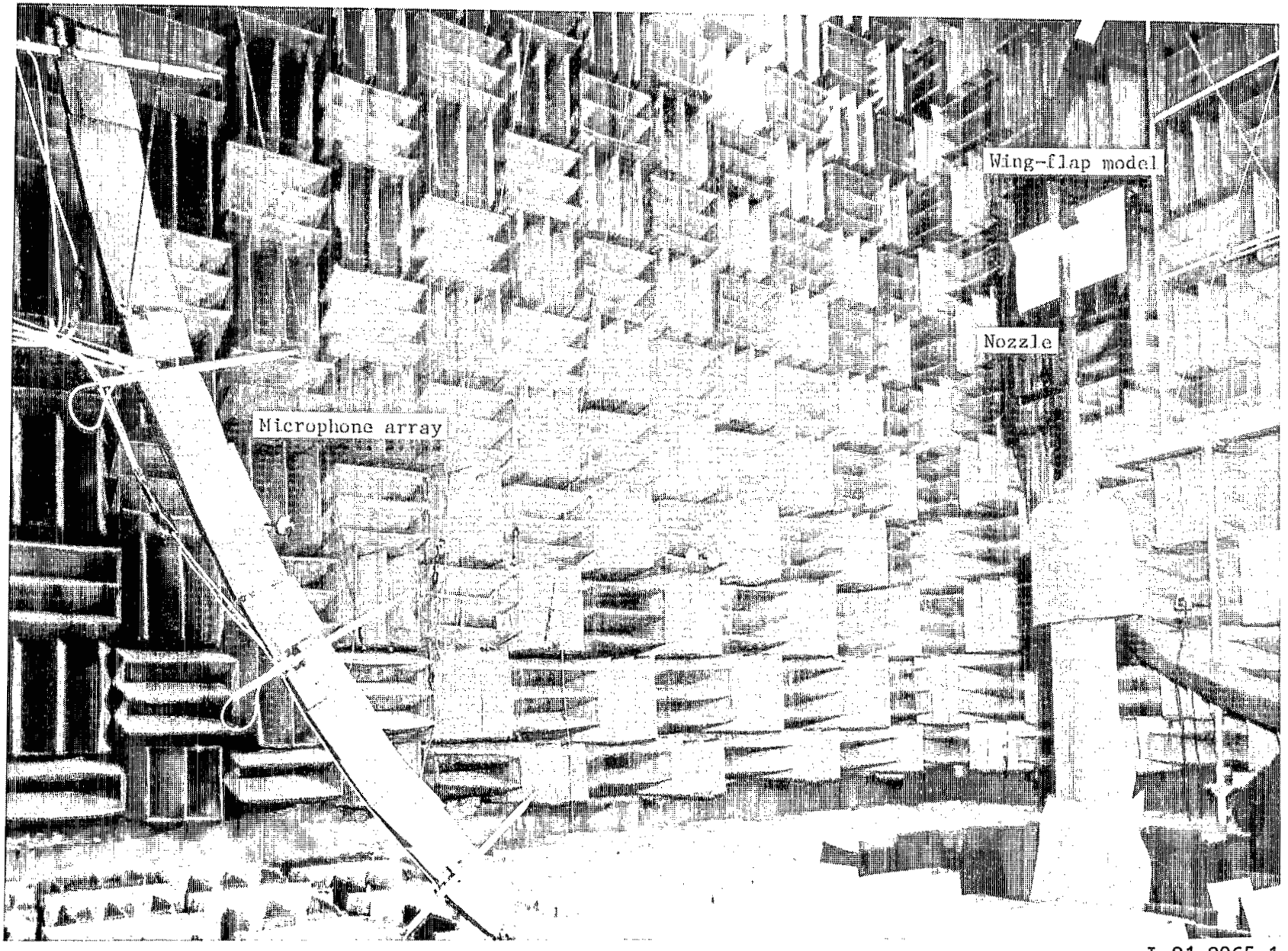

Figure 1.- Photograph of test setup.

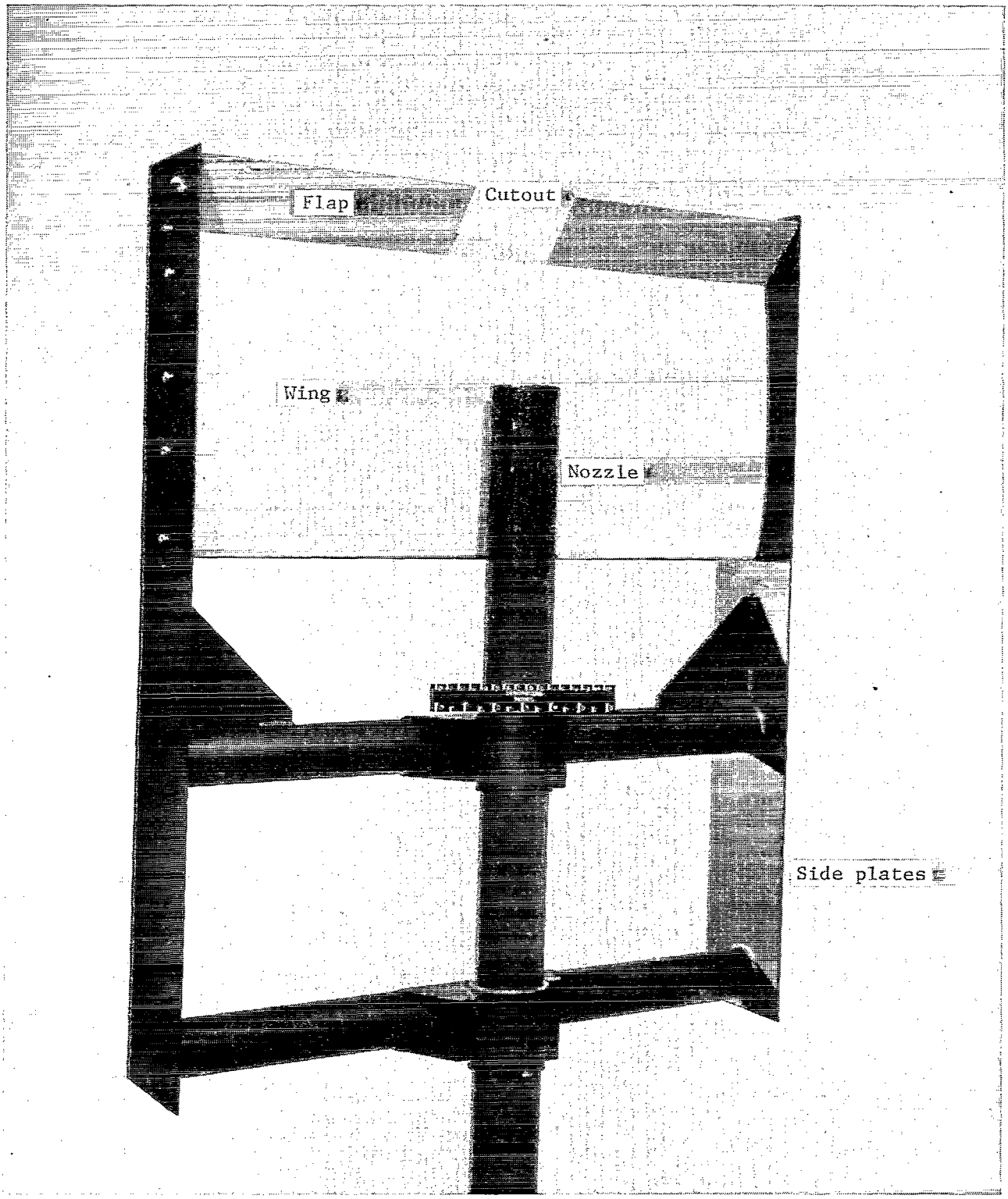

L-81-2425.1

Figure 2.- Photograph of test model.

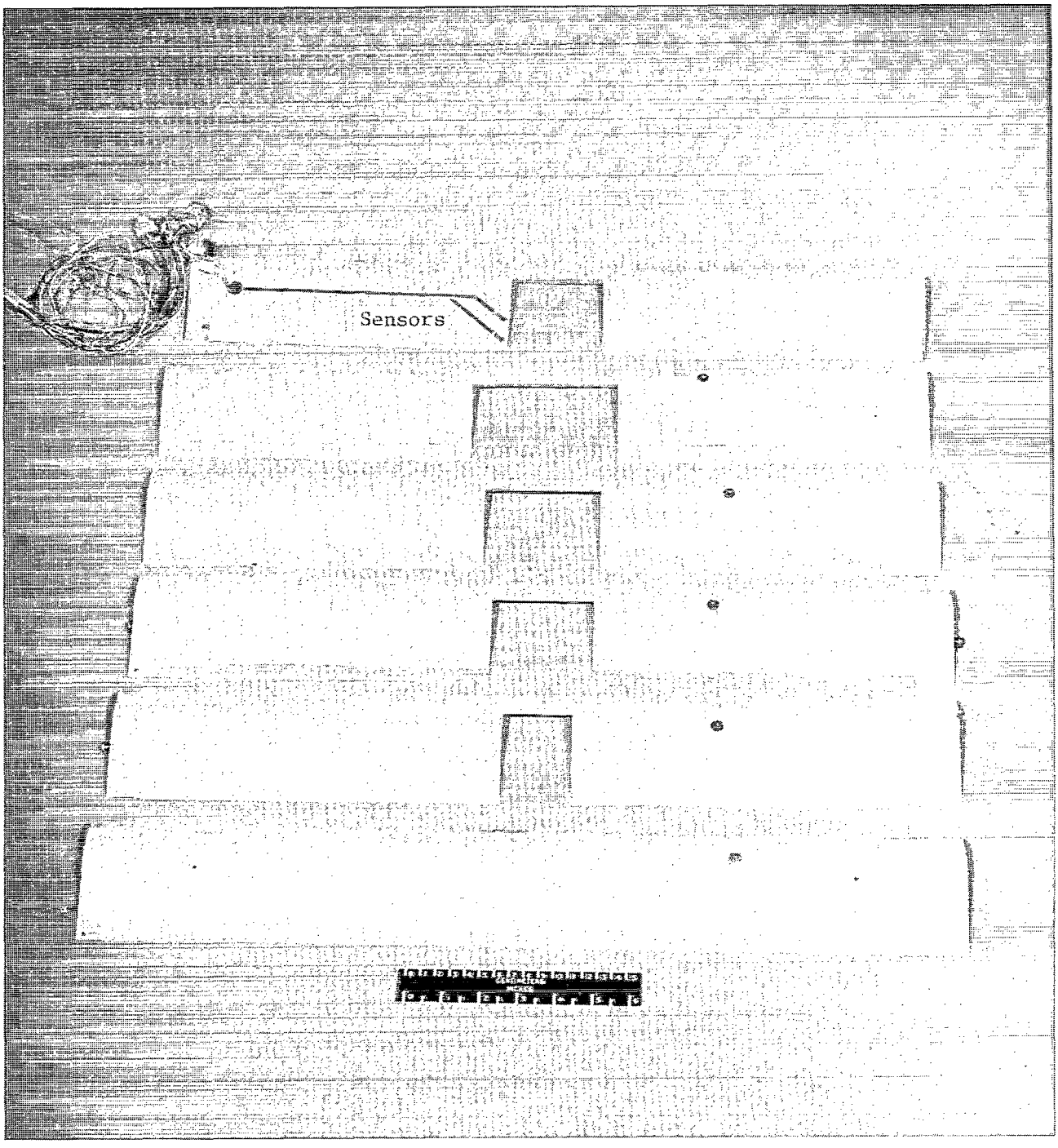

L-81-8967.1

Figure 3.- Photograph of flaps with cutouts.

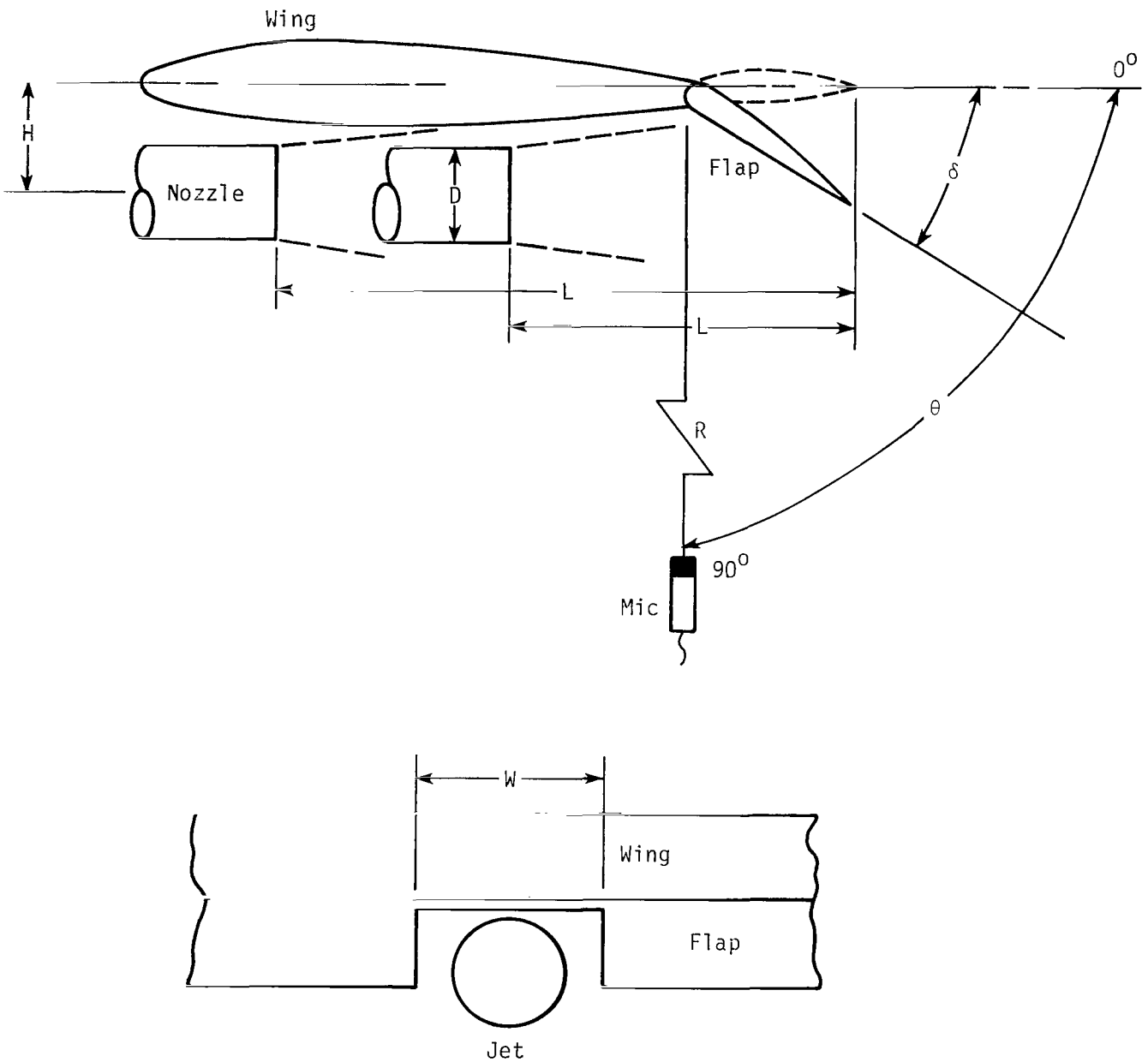

Figure 4.- Schematic diagram of wing-flap model.

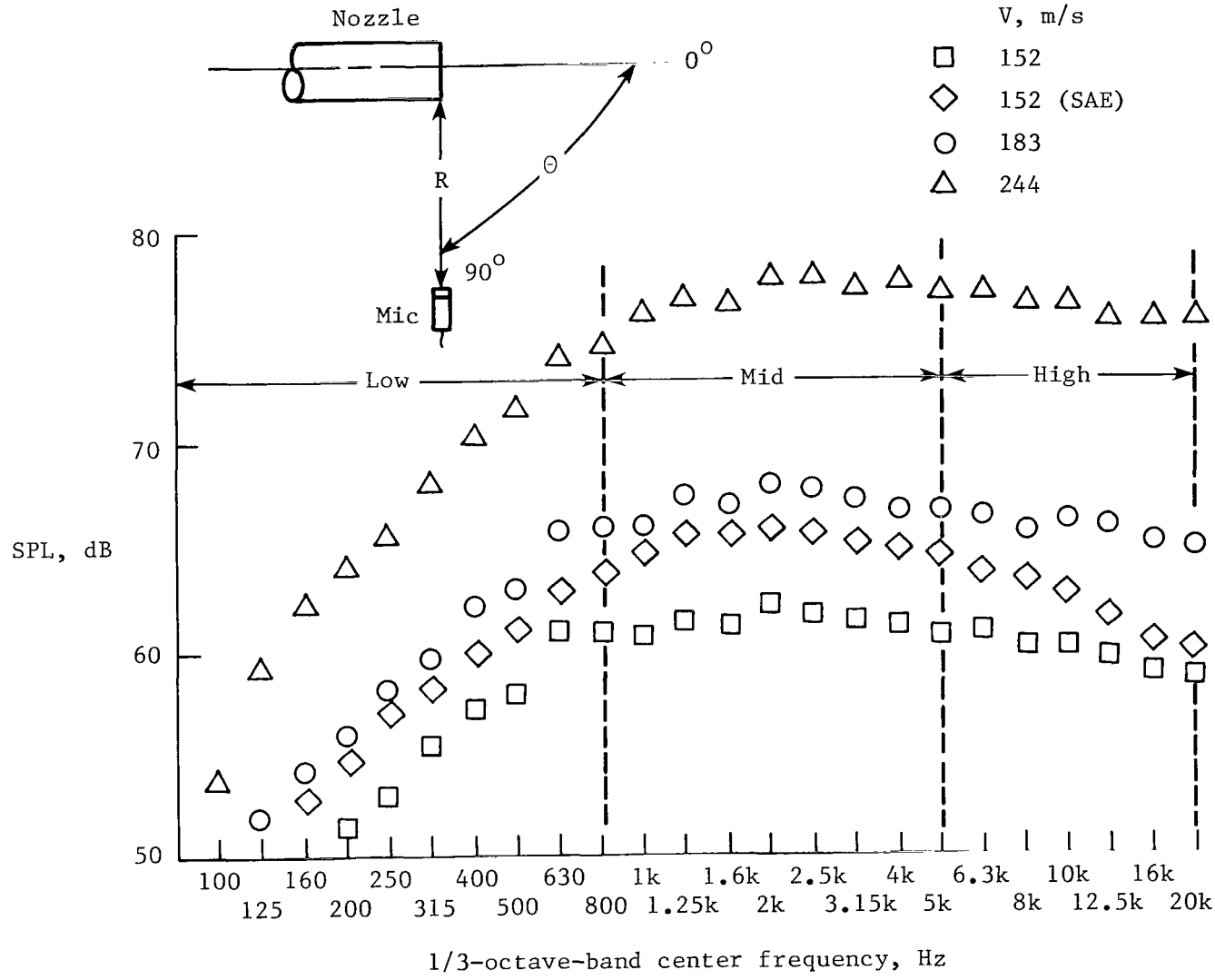

Figure 5.- Free-jet noise spectra.

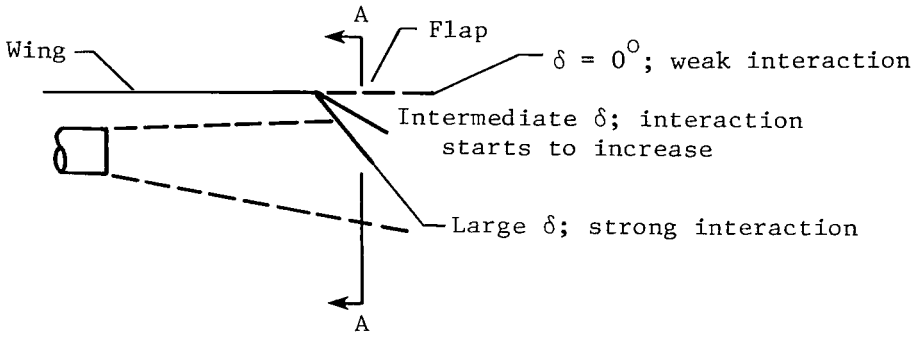

View AA

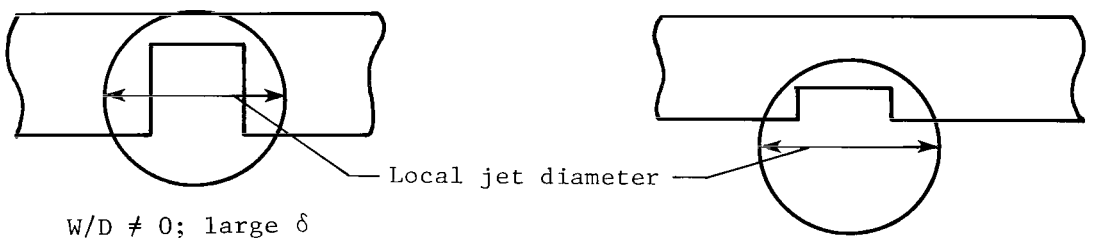

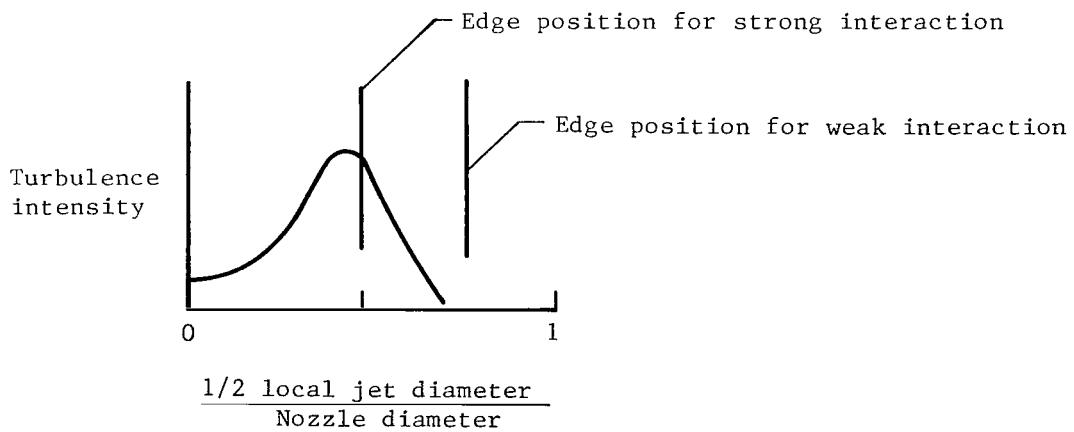

Figure 6.- Schematic diagram of flap location relative to typical turbulent jet.

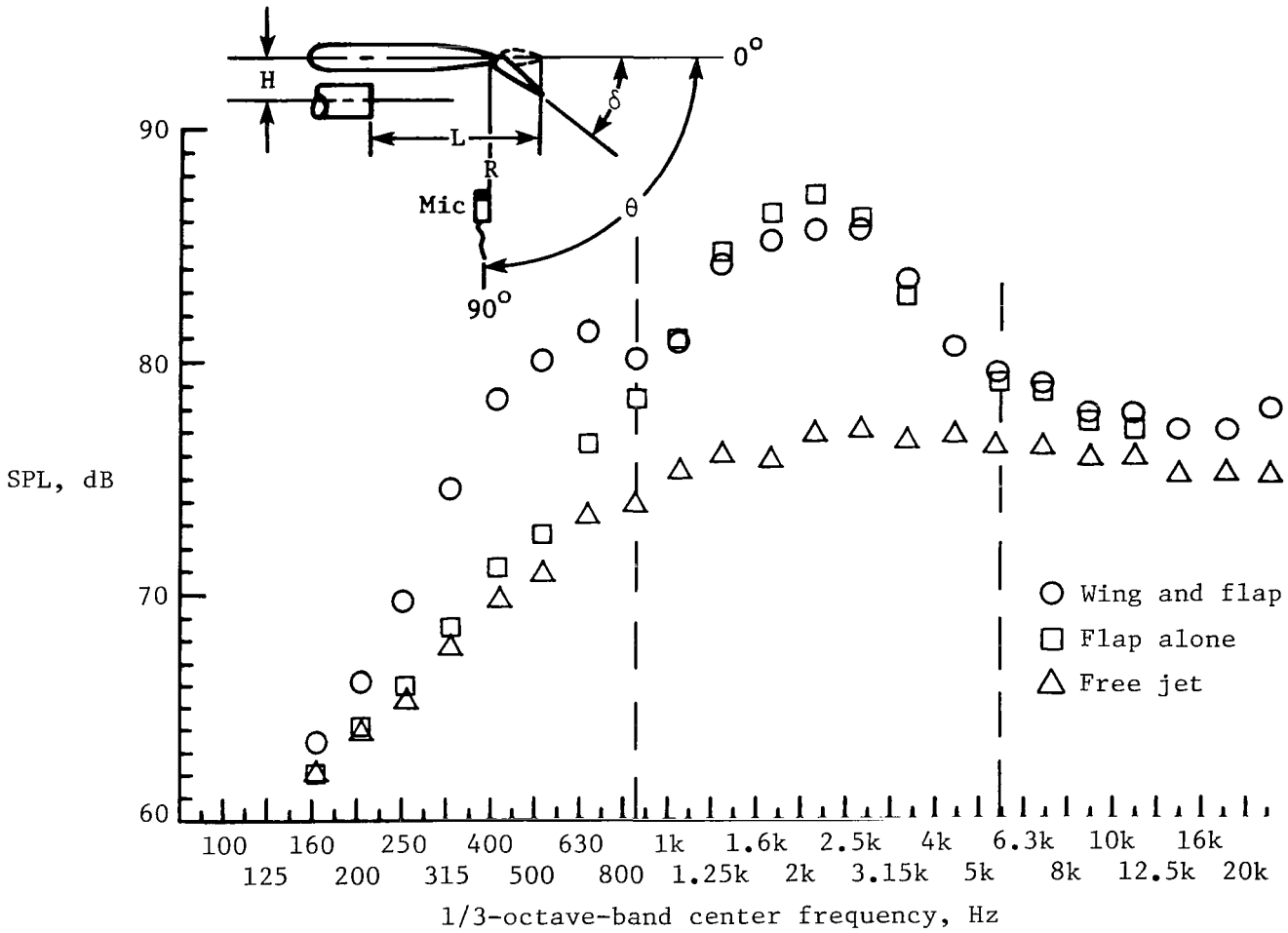

Figure 7.- Wing effects and flap effects on noise spectra at V = 244 m/s. H/D = 1; L/D = 3.6; W/D = 1.3; δ = 40°; θ = 90°.

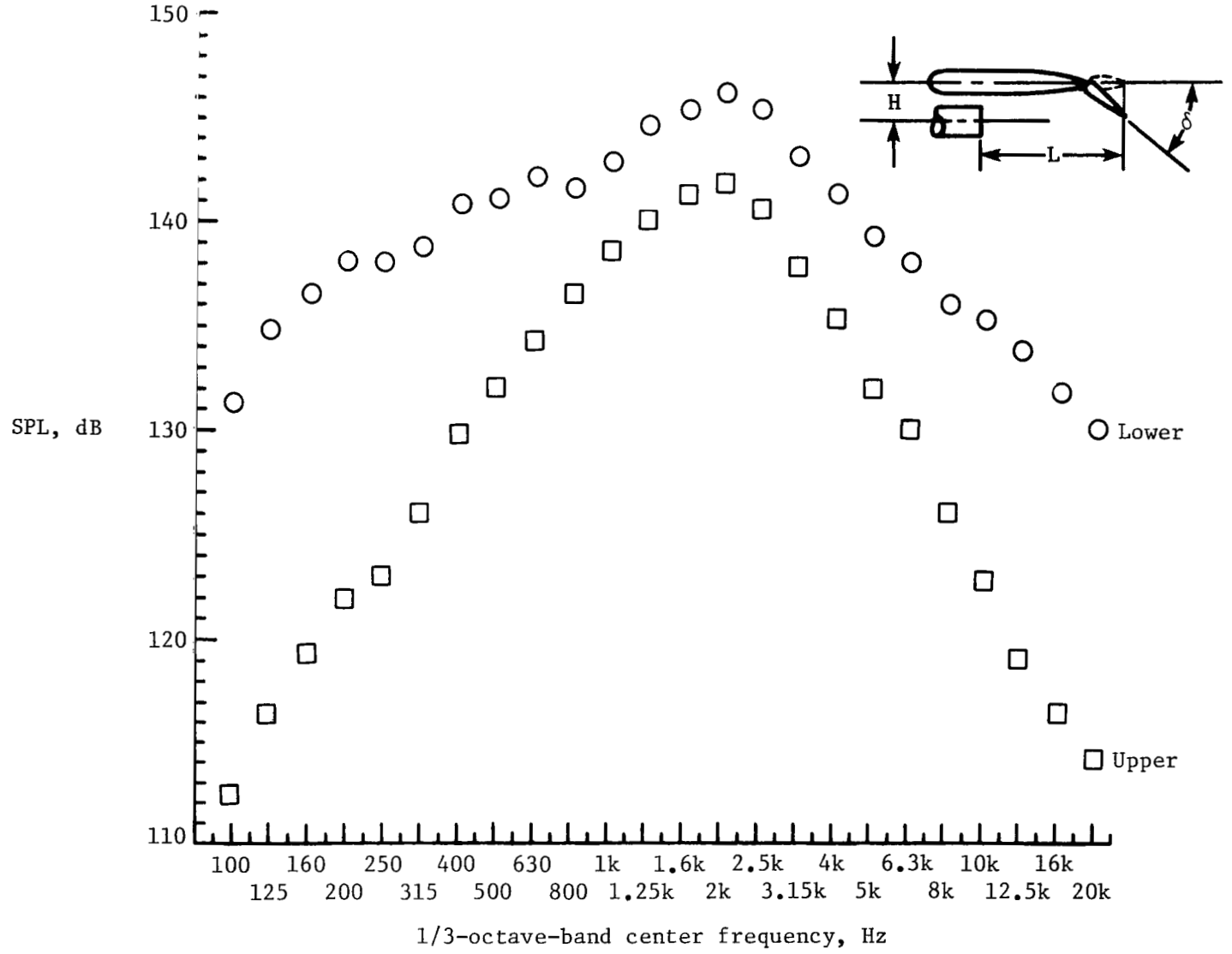

Figure 8.- Pressure spectra measured by flush-mounted pressure transducers on upper and lower flap surfaces at V = 244 m/s. H/D = 1; L/D = 3.6; W/D = 1.3; $\delta = 40°$; $\theta = 90°$.

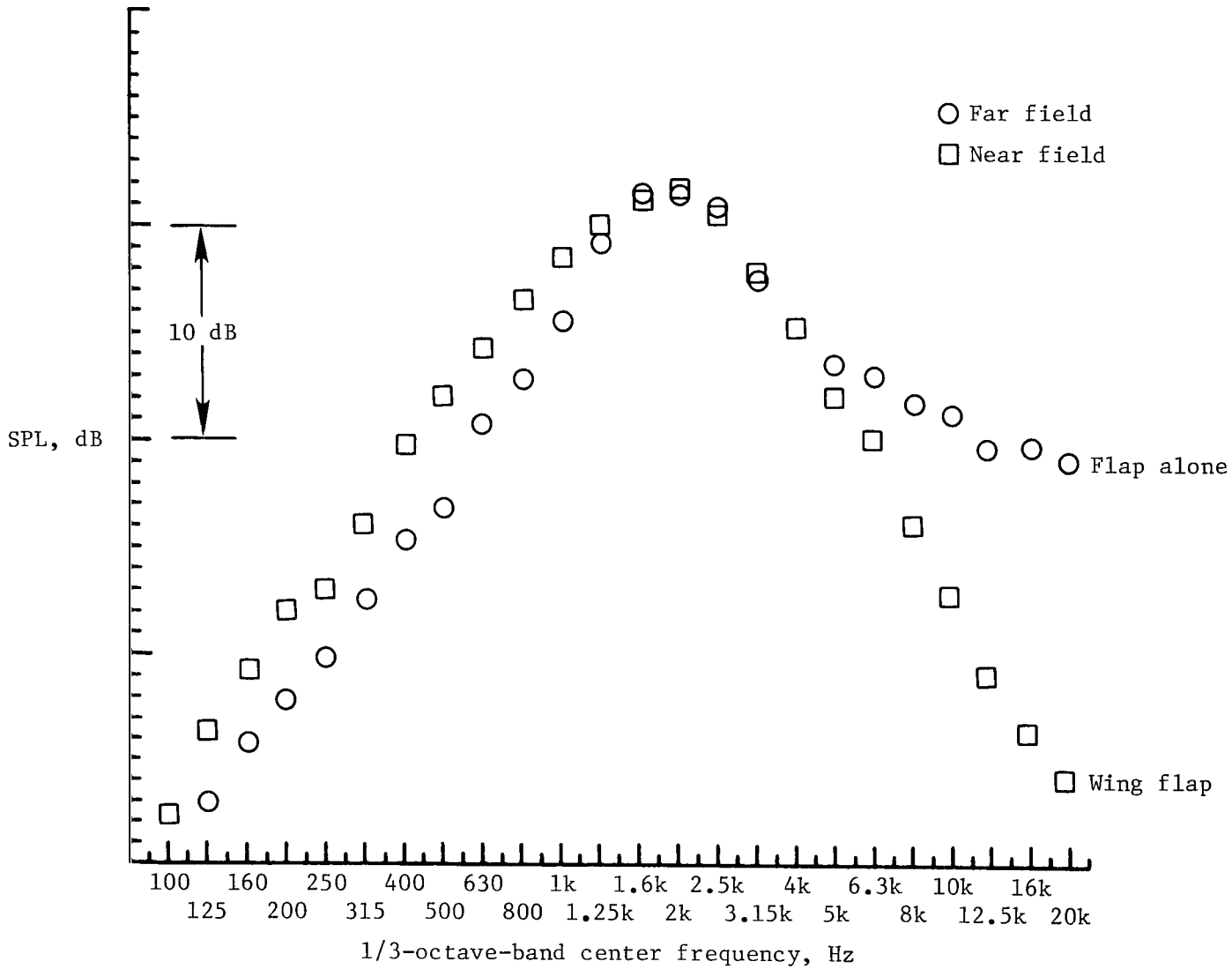

Figure 9.- Superposition of far-field noise spectra of jet and flap alone on upper-surface pressure spectra with jet, wing, and flap at V = 244 m/s. H/D = 1; L/D = 3.6; W/D = 1.3; δ = 40°.

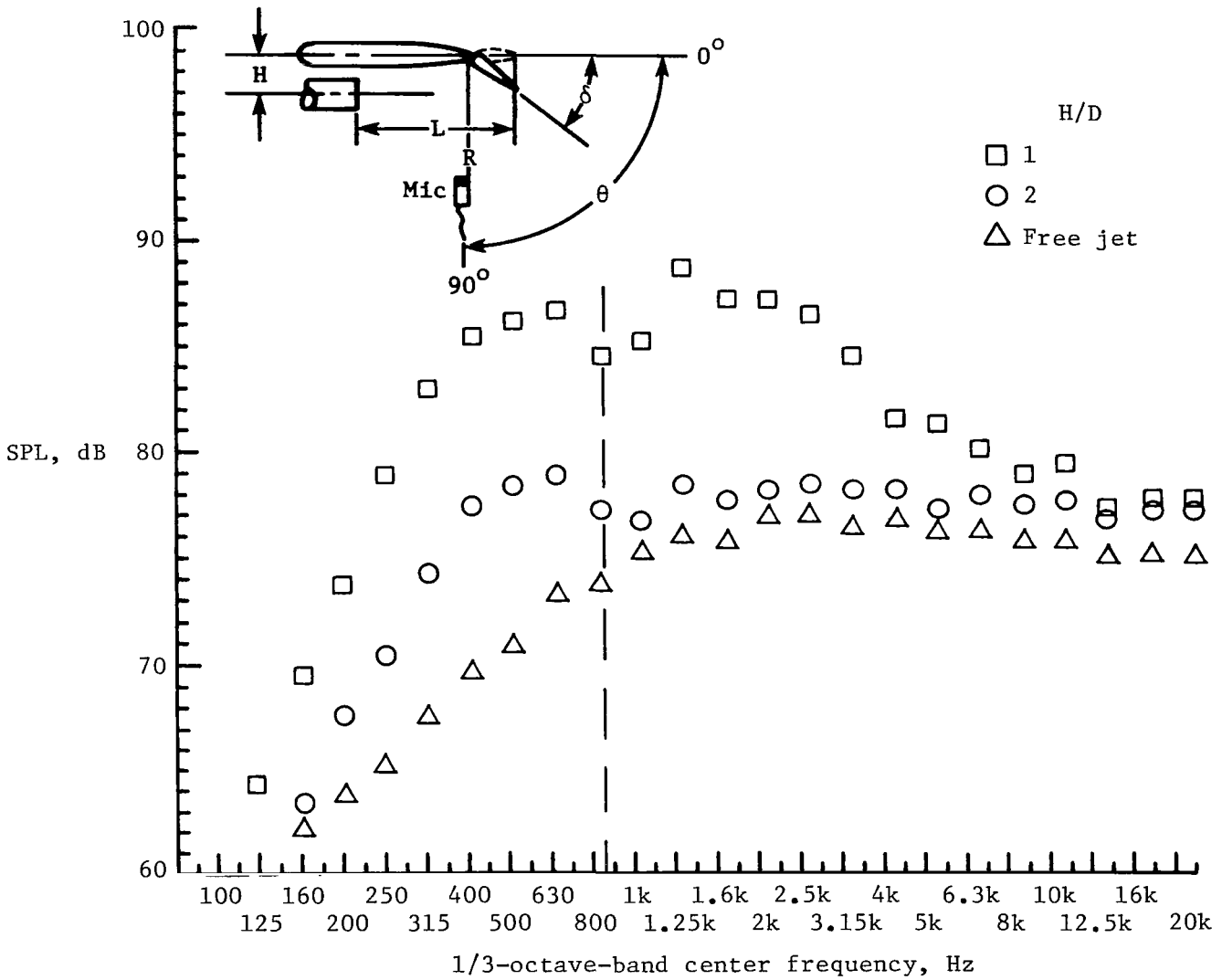

Figure 10.- Effects of normal separation distance on low-frequency-region noise for $\delta = 40°$ at V = 244 m/s. H/D, variable; L/D = 5.5; W/D = 1.3; $\theta = 90°$.

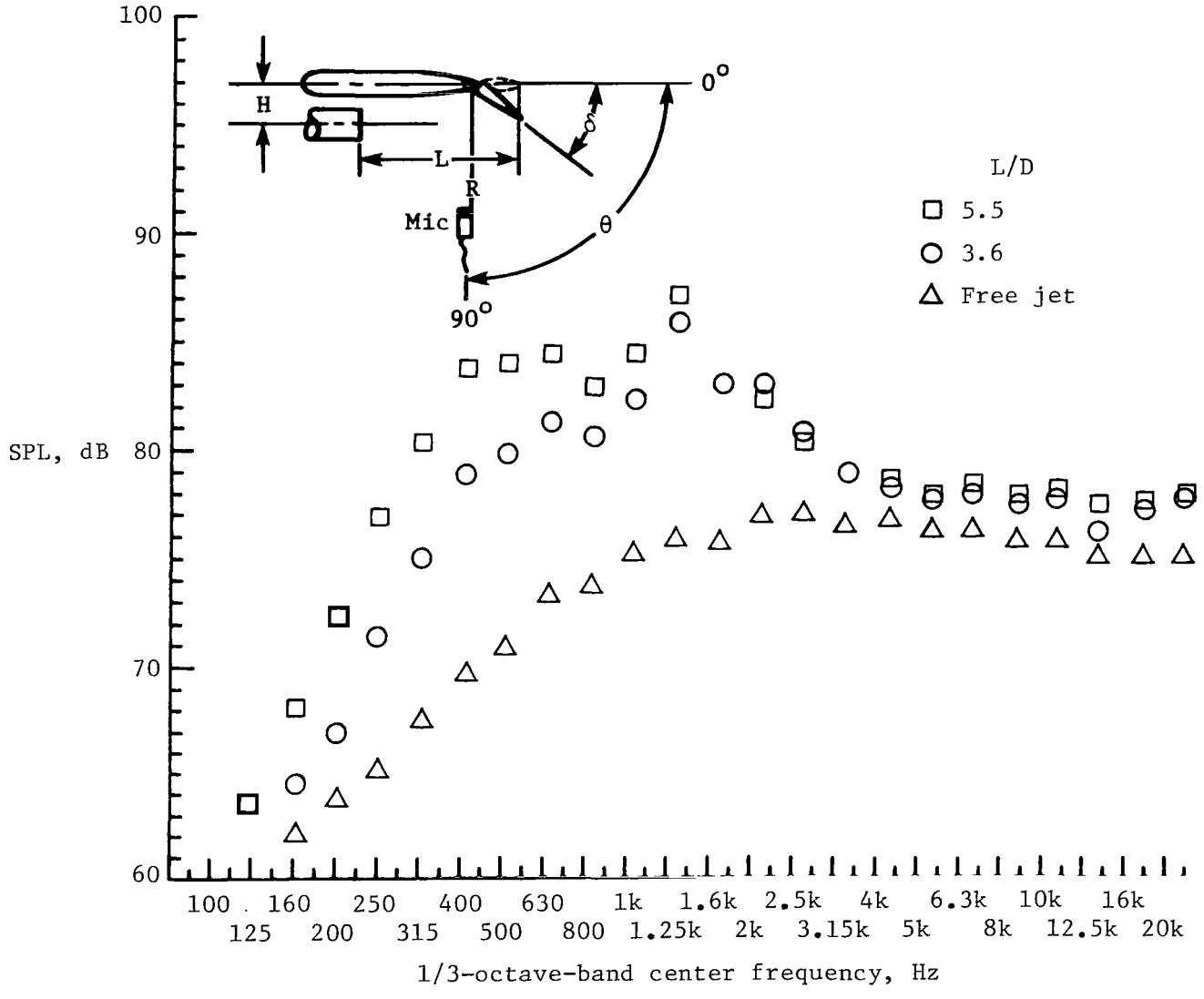

Figure 11.- Dependency of SPL in low-frequency region on separation distance L at V = 244 m/s. H/D = 1; L/D, variable; W/D = 0; δ = 0°; θ = 90°.

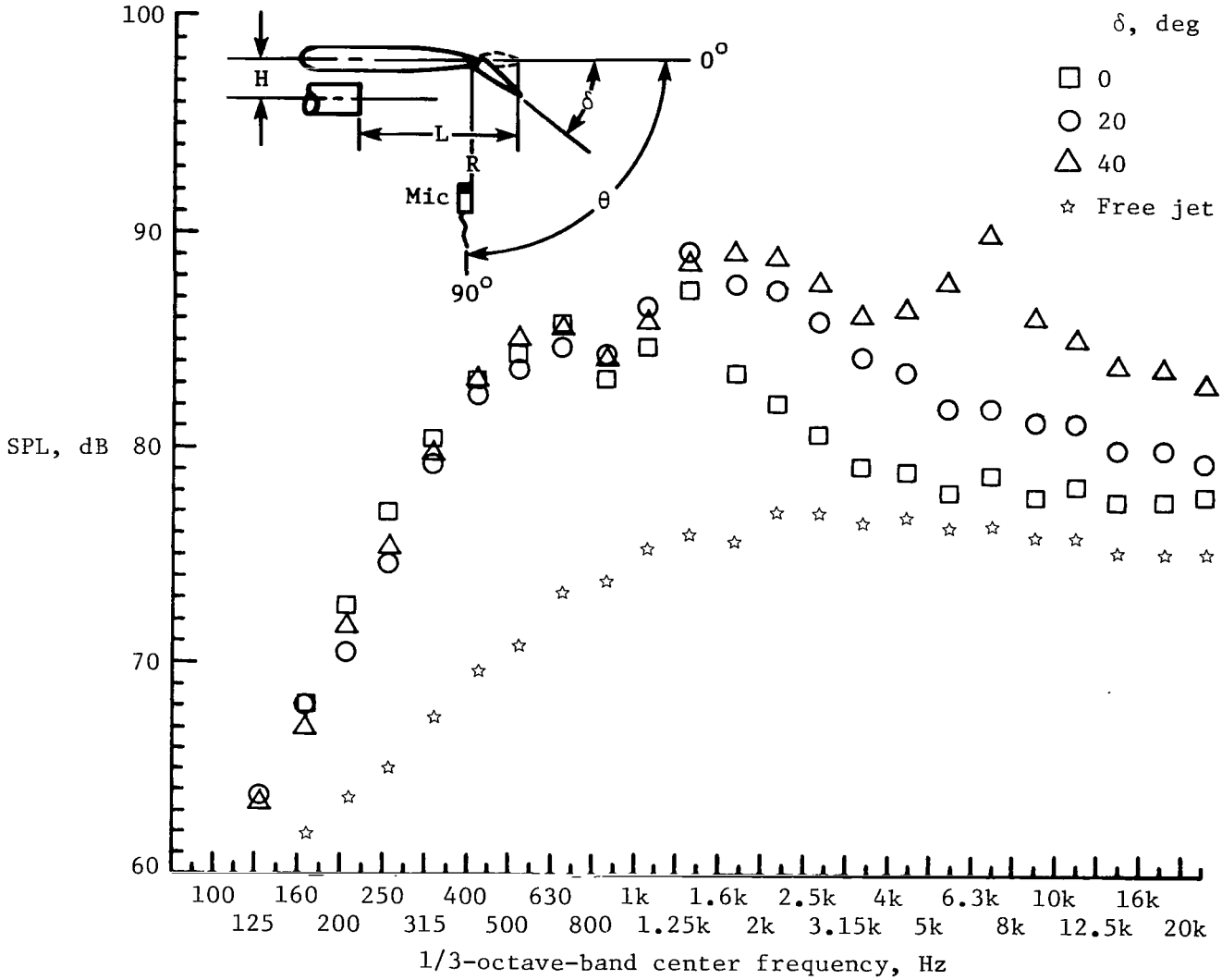

Figure 12.- Effect of flap-deflection angle on noise in low- and high-frequency regions at V = 244 m/s. H/D = 1; L/D = 5.5; W/D = 0; δ, variable; θ = 90°.

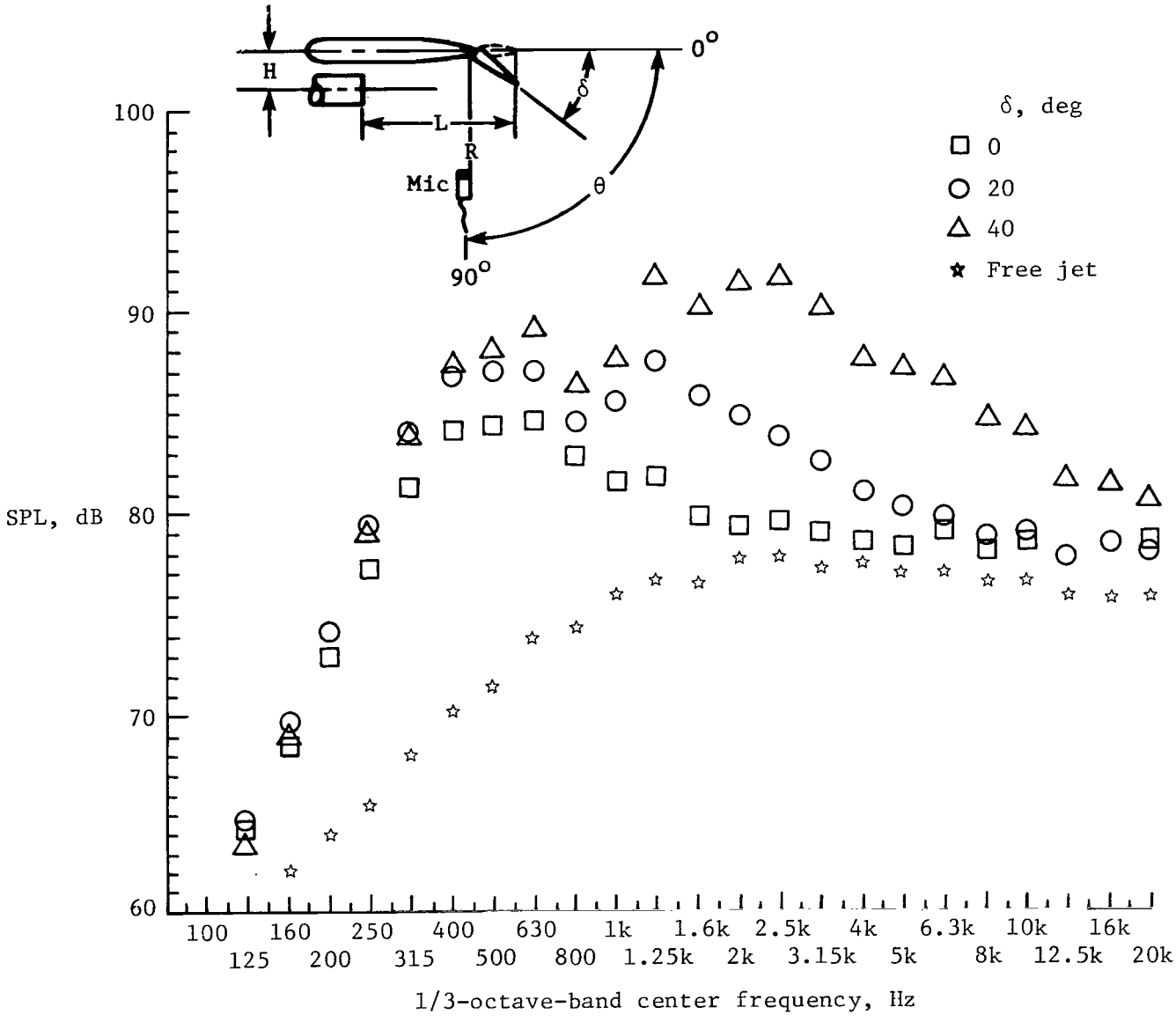

Figure 13.- Effect of flap-deflection angle on 1/3-octave-band noise spectra for W/D = 0.84 at V = 244 m/s. H/D = 1; L/D = 5.5; δ, variable; θ = 90°.

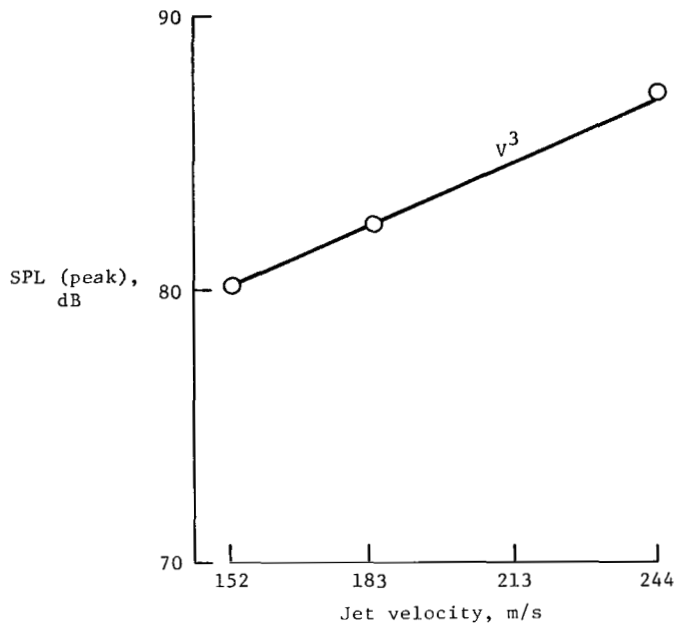

Figure 14.- Effect of jet velocity on peak sound pressure level in low-frequency region. H/D = 1; L/D = 3.6; W/D = 0; δ = 40°; θ = 90°.

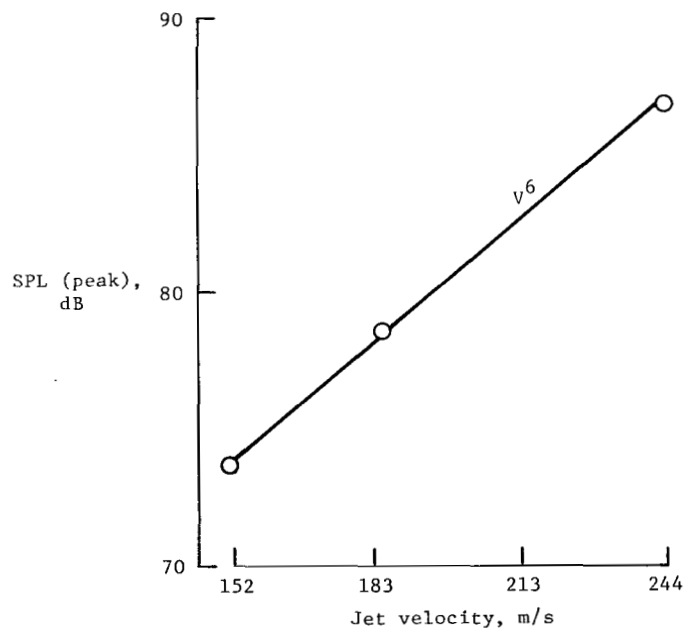

Figure 15.- Effect of jet velocity on peak sound pressure level in midfrequency region. H/D = 1; L/D = 3.6; W/D = 1.3; δ = 40°; θ = 90°.

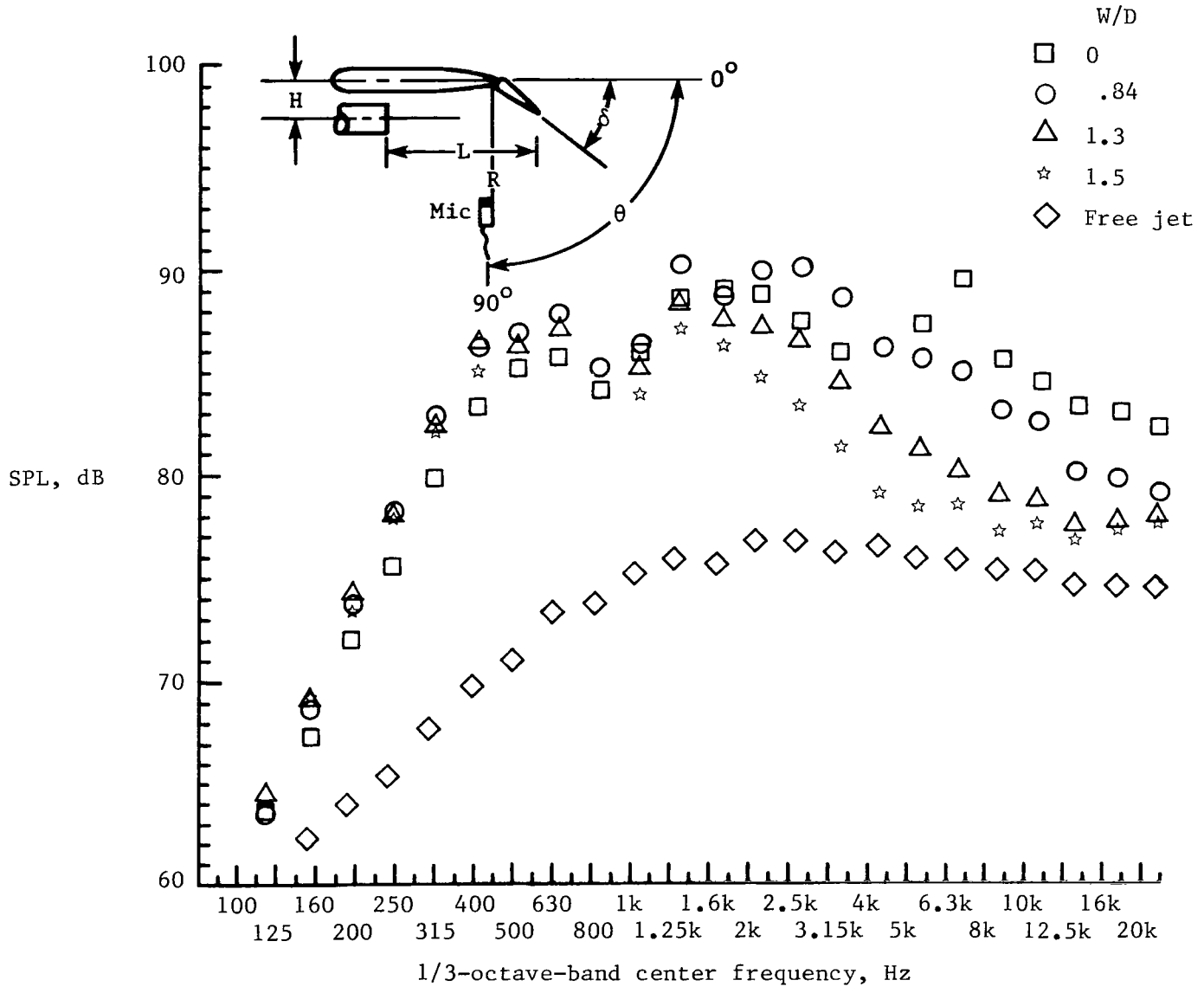

Figure 16.- Midfrequency noise due to interaction of jet flow and side edges of flap cutouts at V = 244 m/s. H/D = 1; L/D = 5.5; W/D, variable; δ = 40°; θ = 90°.

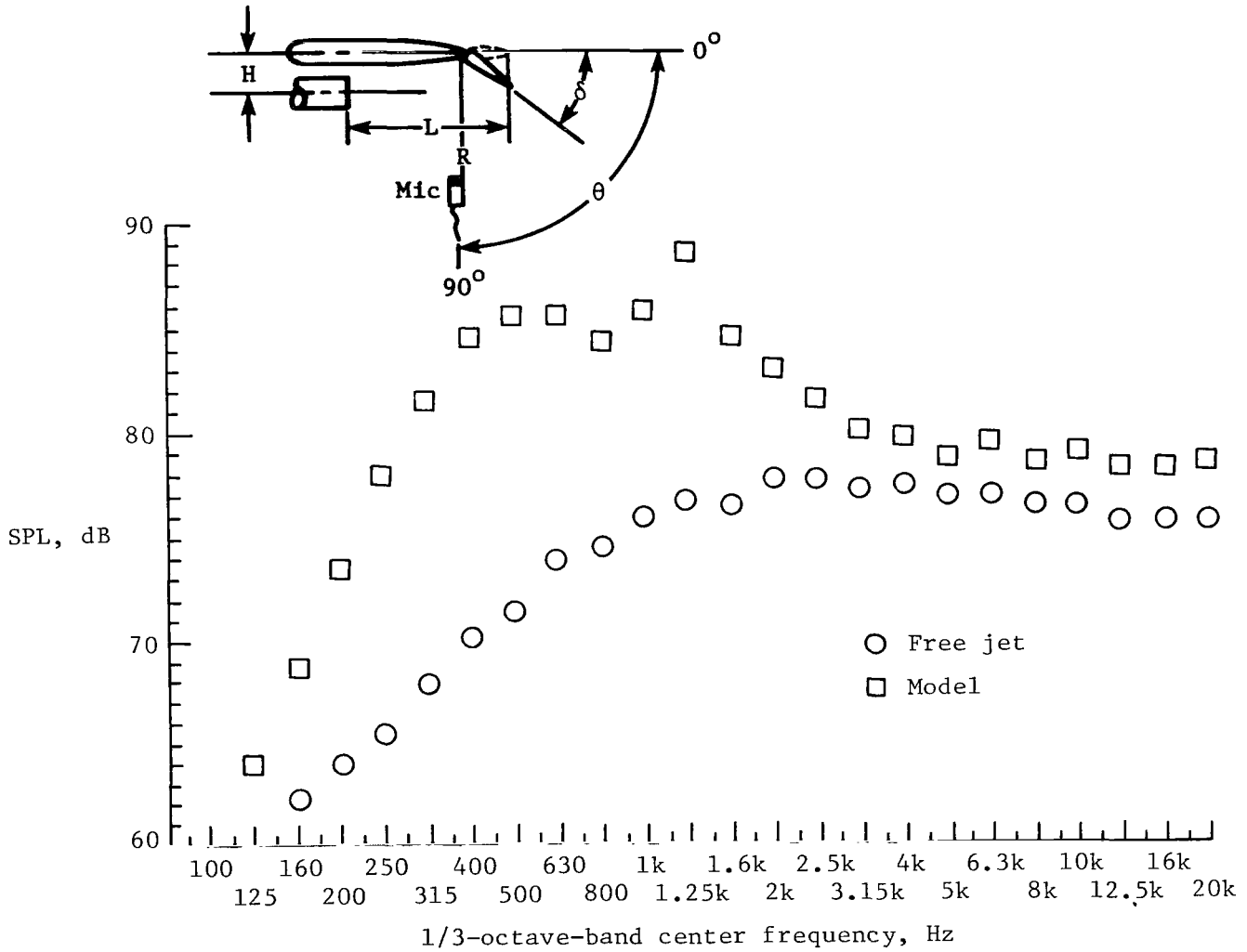

Figure 17.- High-frequency reflections of jet noise at V = 244 m/s. H/D = 1; L/D = 5.5; W/D = 0; δ = 0°; θ = 90°.

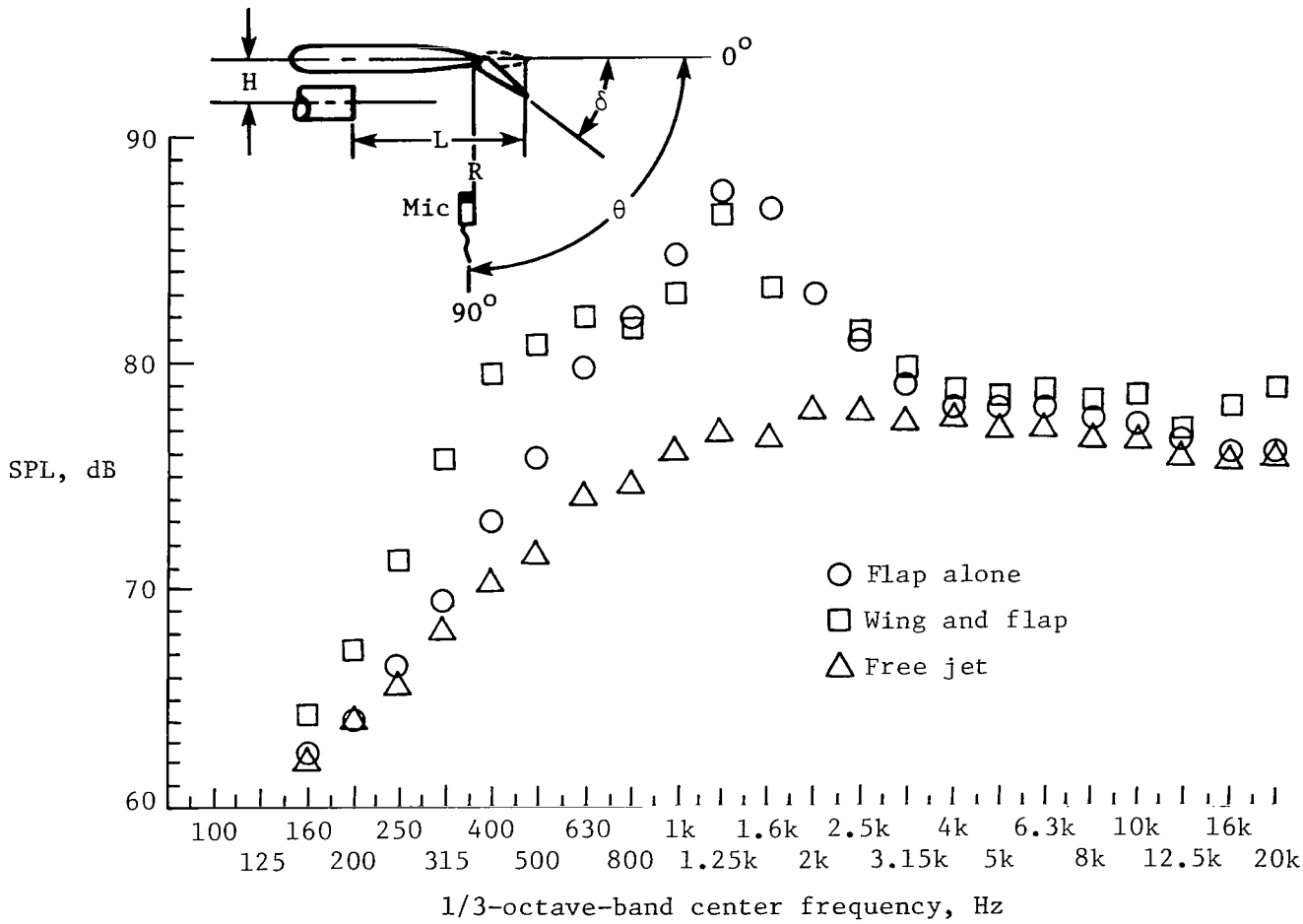

Figure 18.- Comparison of high-frequency-region noise for wing and nondeflected flap and for flap alone with no cutout at V = 244 m/s. H/D = 1; L/D = 3.6; W/D = 0; $\delta = 0°$; $\theta = 90°$.

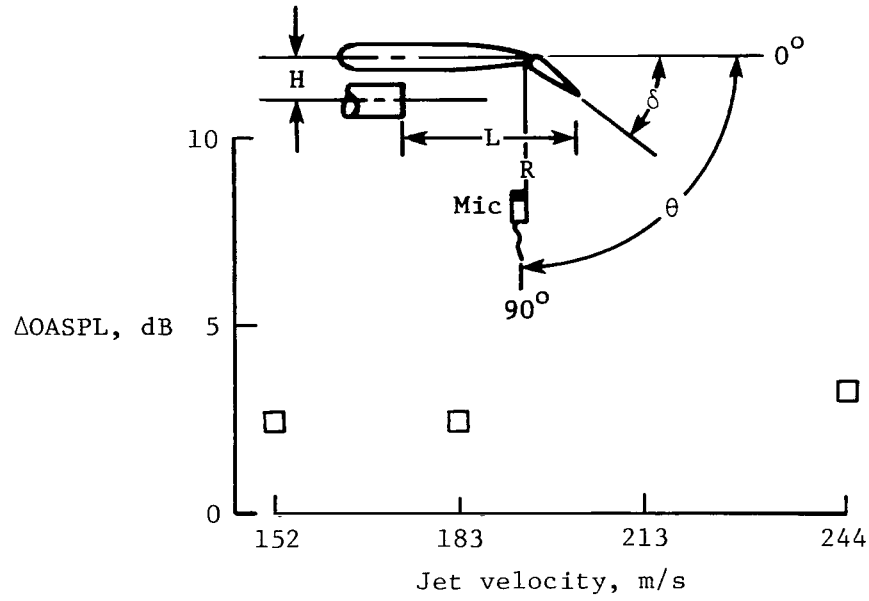

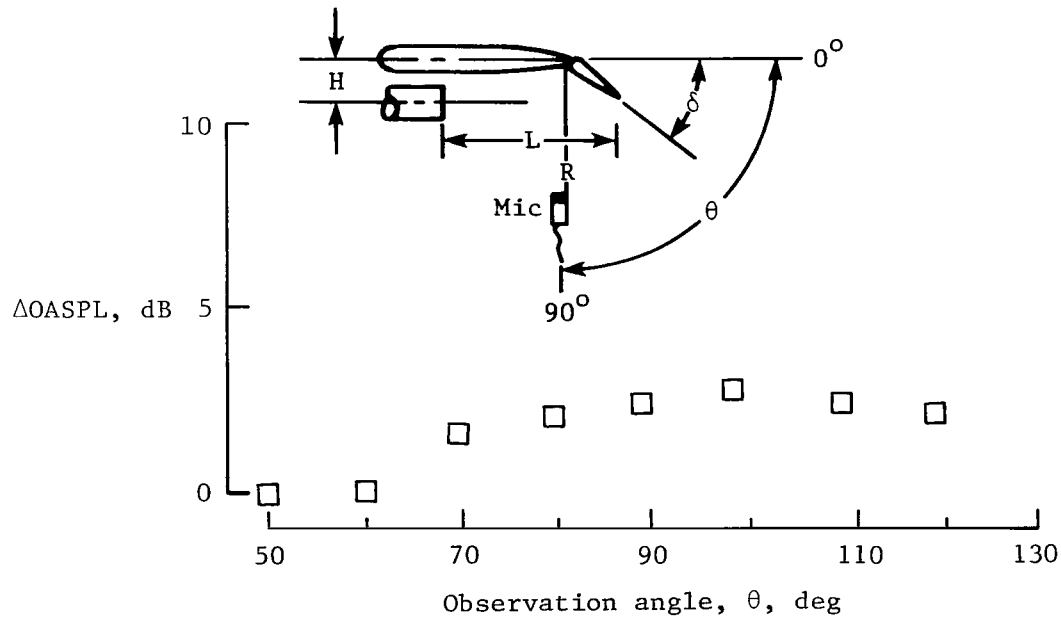

Figure 19.- Dependency of reflected jet noise on jet velocity and observation angle. H/D = 1; L/D = 5.5; W/D = 0; δ = 0°; θ = 90°; V = 244 m/s.

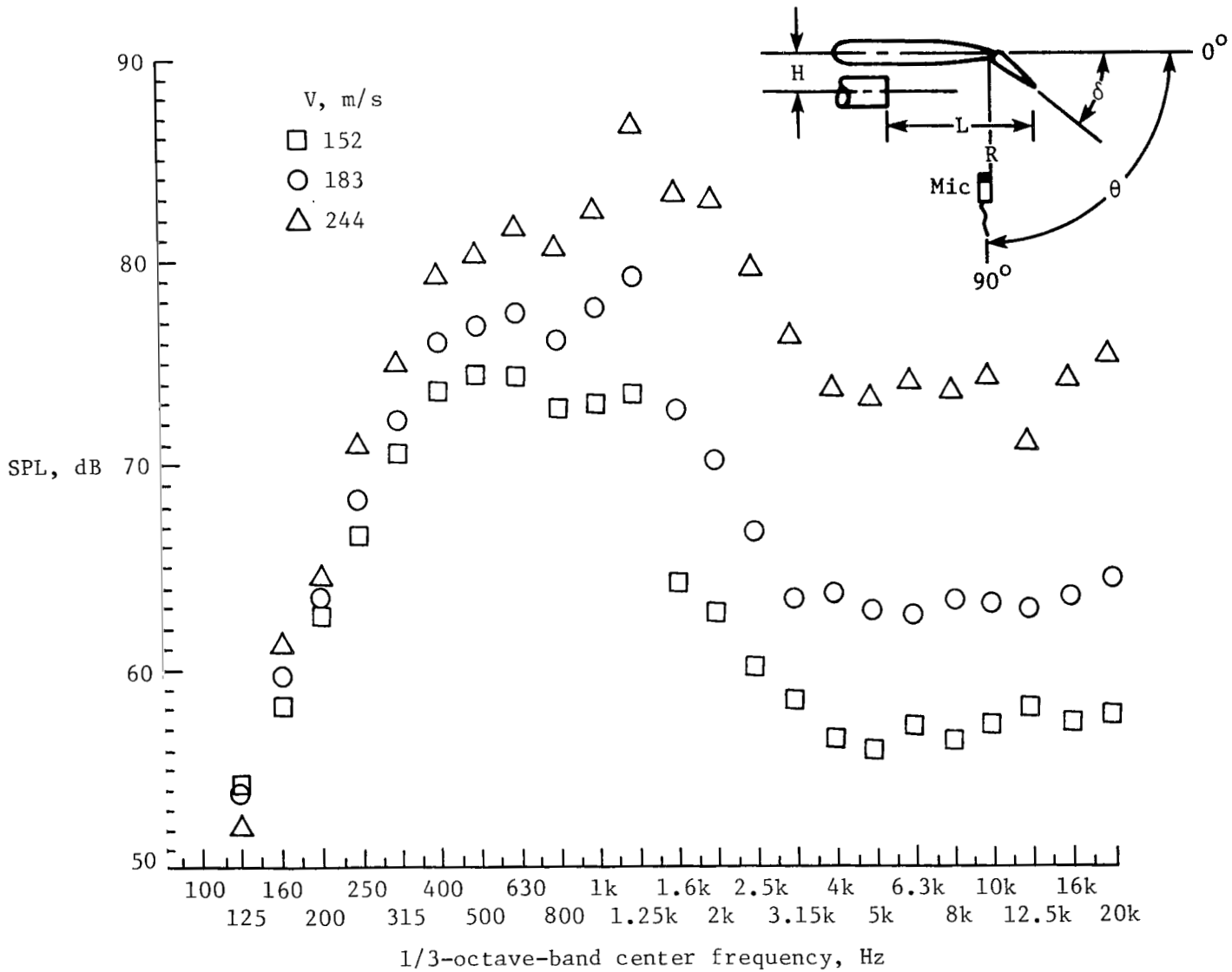

Figure 20.- Noise spectra for wing with nondeflected flap with jet-velocity variation. H/D = 1; L/D = 3.6; W/D = 0; δ = 0°; θ = 90°.

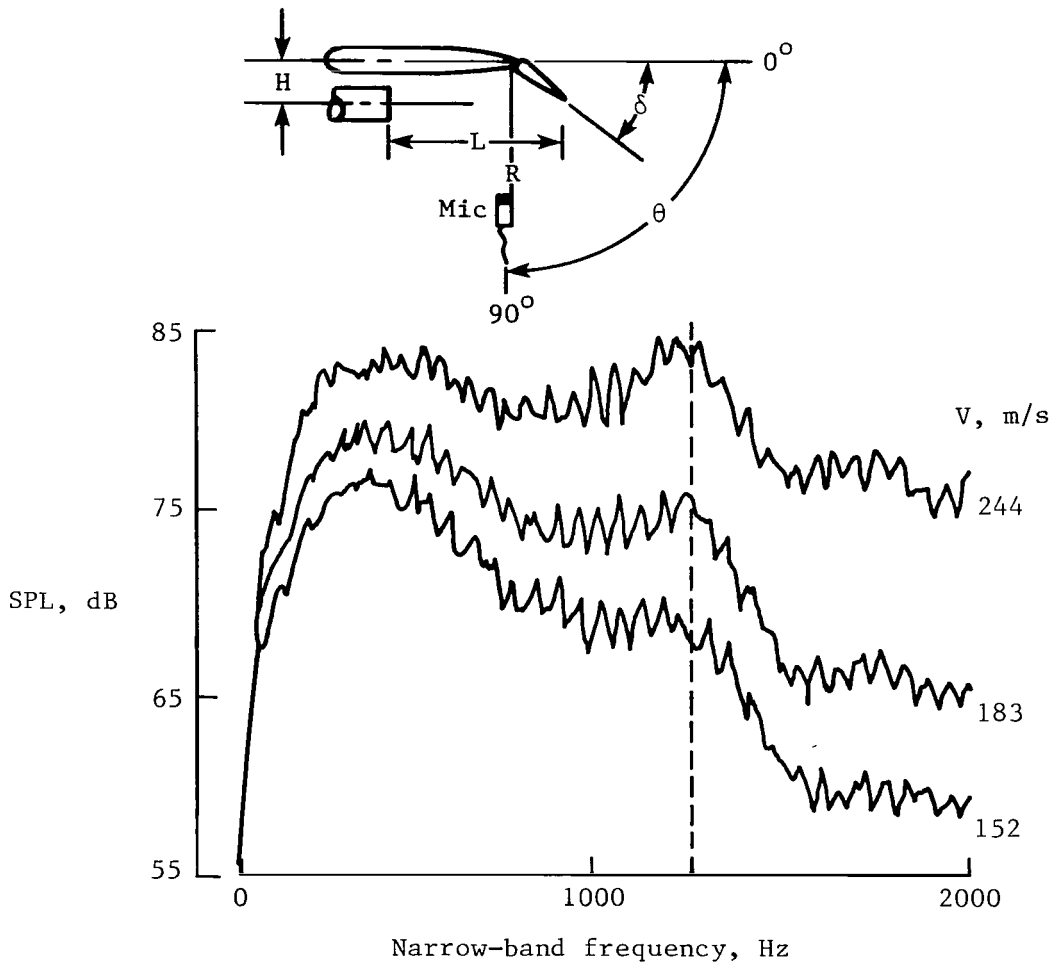

Figure 21.- Analysis of narrow-band frequency of noise due to wing with nondeflected flap. H/D = 1; L/D = 5.5; W/D = 0; δ = 0°; θ = 90°.

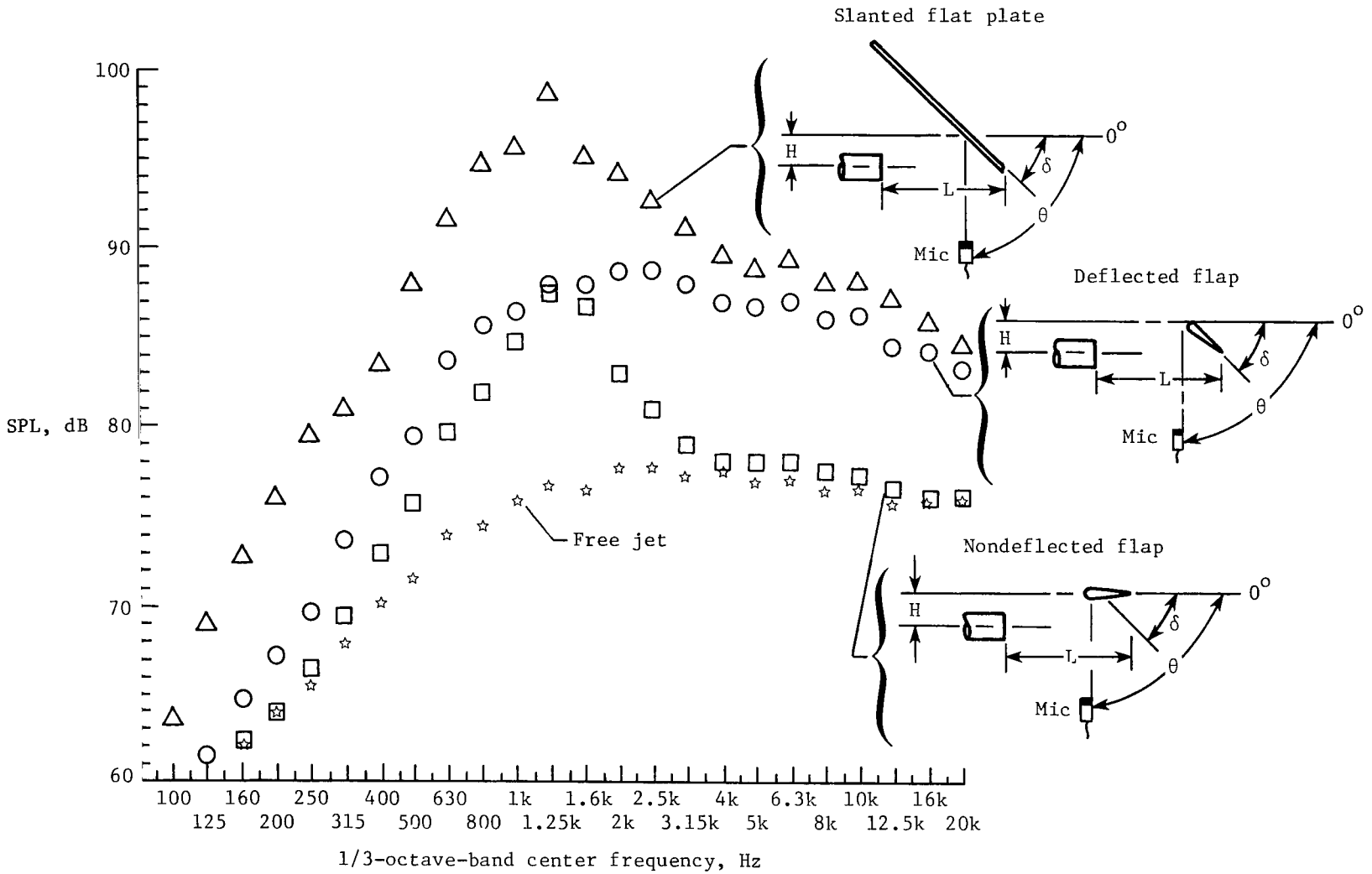

Figure 22.- Noise spectra of slanted flat plate, deflected flap, and nondeflected flap at V = 244 m/s. H/D = 1; L/D = 3.6; W/D = 0; δ, variable; θ = 90°.

1. Report No.	2. Government Accession No.	3. Recipient's Catalog No.
NASA TP-2181		

4. Title and Subtitle
INVESTIGATION OF JET-INSTALLATION NOISE SOURCES UNDER STATIC CONDITIONS

5. Report Date
August 1983

6. Performing Organization Code
505-31-33-12

7. Author(s)
John G. Shearin

8. Performing Organization Report No.
L-15599

9. Performing Organization Name and Address
NASA Langley Research Center
Hampton, VA 23665

10. Work Unit No.

11. Contract or Grant No.

12. Sponsoring Agency Name and Address
National Aeronautics and Space Administration
Washington, DC 20546

13. Type of Report and Period Covered
Technical Paper

14. Sponsoring Agency Code

15. Supplementary Notes

16. Abstract

The acoustical effects of operating a 6-cm exit-diameter nozzle in the presence of a wing-flap model under static conditions are examined experimentally. The geometric parameters of the wing-flap model are chosen to represent a realistic jet-engine installation on a wide-body midrange transport airplane. The effects of varying the installation parameters and the noise sources associated with the engine-installation effects are discussed. The major noise sources are the flow interaction of the jet and wing undersurface, the flow interaction of the jet with the side edges of the flap cutout and flap trailing edge, and the reflection of the jet noise off the undersurface of the wing and flap.

17. Key Words (Suggested by Author(s))	18. Distribution Statement
Jet-installation noise Aeroacoustics Jet-flap-interaction noise	Unclassified - Unlimited Subject Category 71

19. Security Classif. (of this report)	20. Security Classif. (of this page)	21. No. of Pages	22. Price
Unclassified	Unclassified	31	A03

For sale by the National Technical Information Service, Springfield, Virginia 22161

NASA-Langley, 1983

National Aeronautics and
Space Administration

Washington, D.C.
20546

Official Business
Penalty for Private Use, $300

THIRD-CLASS BULK RATE

Postage and Fees Paid
National Aeronautics and
Space Administration
NASA-451

6 1 1U,H, 830830 S00903DS
DEPT OF THE AIR FORCE
AF WEAPONS LABORATORY
ATTN: TECHNICAL LIBRARY (SUL)
KIRTLAND AFB NM 87117

NASA

POSTMASTER: If Undeliverable (Section 158 Postal Manual) Do Not Return